Vol. 9 Issue 9 September - 2025, Pages: 1-12

Rheological Characterization of Thermoplastic Polymers Using Melt Flow Index: Viscosity Modeling of LDPE and PP

¹Yousif.A A,²Maysa.E.M. ³Mohamad H. H. Deifalla

1,2,3 Sudan University of Science and Technology
1,2 Polymer Engineering Department, ³ Chemical Engineering Department
1,2,3 Sudan .Khartoum

¹abdalbagyyousif@gmail.com, mohammed.hassan.eng@gmail.com

Abstract— This work presents a rheological investigation of thermoplastic polymers using melt flow index (MFI) testing, focusing on low-density polyethylene (LDPE) and polypropylene (PP). Measurements of MFI and melt volume rate (MVR) were conducted at different temperatures and applied loads with a capillary plastometer. The experimental data were used to calculate shear stress, shear rate, viscosity, and mass flow. Results revealed that viscosity decreased with increasing temperature and MFI, confirming the pseudo plastic nature of both polymers. The rheological behavior was successfully modeled using the Power Law and Carreau models, with power-law indices (n) ranging between 0.58–0.61 for LDPE and 0.60–0.66 for PP. Activation energies were also determined, highlighting the thermal sensitivity of melt viscosity. Overall, the study demonstrates the effectiveness of MFI testing as a practical tool for correlating viscosity with processing parameters, providing valuable insights for optimizing thermoplastic polymer processing in industrial applications.

Keywords: Melt flow index, Rheology, LDPE, Polypropylene, Viscosity, Non-Newtonian behavior.

1. INTRODUCTION

most widely processed materials due to their excellent balance of mechanical, thermal, and economic properties. Understanding their rheological behavior is critical for optimizing processing conditions, predicting end-use performance, and ensuring product quality. Among the commonly used rheological parameters, the melt flow index (MFI), measured under standardized conditions, remains a widely adopted empirical indicator of polymer processability and molecular characteristics. Although MFI does not represent a fundamental property, it provides a convenient means to assess viscosity-related behavior and serves as a practical tool for material selection and quality control [1].

Recent years have seen growing interest in refining the correlation between MFI, shear viscosity, and molecular structure. For example, predictive modeling approaches have been developed to relate MFI with viscosity and molecular weight distribution in PP blends, improving the reliability of MFI as a processing predictor [2]. Similarly, studies on recycled PP have shown that operational parameters significantly influence both MFI and viscosity, underlining the importance of rheological monitoring in sustainable polymer processing [3]. Other research demonstrated that chain extension and radiation treatment can tailor the viscosity of post-consumer PP, with MFI reduction reflecting enhanced molecular entanglement [2].

For polyethylene systems, solvent-based recycling processes have been assessed in terms of shear and extensional rheology, confirming that changes in MFI correspond to measurable variations in flow curves and viscosity profiles[4]. Complementary experimental work on HDPE and PP extrusion reported non-Newtonian pseudoplastic behavior, which was successfully modeled using power-law relationships, highlighting the connection between experimental MFI and theoretical viscosity laws [5]. Moreover, feasibility studies on producing low-MFR PP further illustrated the industrial relevance of tailoring MFI to achieve desired mechanical and rheological performance [6].

Building on these advancements, this work aims to investigate the rheological behavior of LDPE and PP using MFI measurements at various temperatures and loads. The study further applies rheological models, including the Power Law and Carreau equations, to correlate experimental data with theoretical predictions, and evaluates the activation energy for viscous flow. The findings are expected to provide practical insights into the use of MFI as a rheological tool for optimizing thermoplastic processing. Polypropylene and polyethylene systems.

Traxler et al. (2024) developed predictive models for MFR and shear viscosity of PP blends using Arrhenius and Cragoe equations, achieving excellent fit $(R^2 > 0.99)[2]$.

Zhiltsova and Oliveira (2025) investigated the balance between recycled content and processing performance, demonstrating predictable MFI trends across blend ratios[7].

Relatedly, al (2024) study on thermomechanical behavior of recycled LDPE and PP from multilayer waste linked extrusion conditions to variations in MFI and mechanical properties.[8] Another investigation into glass-fiber-reinforced recycled PP composites showed a reduction in MFI and a rise in viscosity proportional to filler content[9]

Issues of MFR variability in recyclates and strategies using mixing rules were critically discussed in a 2023 review, emphasizing the need for blend design in industrial recycling. Finally, a kinetic degradation model was proposed linking multiple reprocessing cycles of PP to MFI and molecular weight changes[9].

2-MATERIAL AND METHOD

Material:

Thermoplastic materials used in this study include:

- 1- LDPE (low density polyethylene)(HP 2022: no slip & No Anti block) for blown film from SABIC (**Saudi Arabia Basic Industries corporation**).
- 2- Typical Applications:

Thin shrink film, lamination film, produce bags, textile packing, soft goods packing and general purpose bags with good optics and carrier bags.

Typical data:

Table 1: The basic characteristics of the used material

Properties	unit	Value
Resin properties		
Melt flow rate @190° C&2.16 kg load	g/10 min.	2
Density @ 23 ⁰ C	kg/m³	922
Mechanical Propertie	es .	
Tensile Strength @ break	MPa	21
Tensile Elongation @ break	%	290
Tensile strength @ yield	MPa	8
1% Secant Modulus	MPa	160
Dart Impact Strength	g	60
Elmendorf Tear strength	g	180
Optical Properties		
Haze	%	7
Gloss @ 45 ⁰	-	80
Thermal softening poi		
Vicat softening point	⁰ C	92

Source: Saudi Arabia Basic Industries Corporation (Sabic)

3- Polypropylene(PP)

Method:

Melt Flow rate Index Testing instrument was used. It consists of a heated barrel and piston assembly to contain a sample of resin. A specified load (weight) is applied to the piston, and the melted polymer is extruded through a capillary die of specific dimensions shown in figure .1. The mass of resin, in grams, that is extruded in 10 minutes equals the MFR; expressed in units of g/10 min. Some instruments can also calculate the shear rate, shear stress, and viscosity.

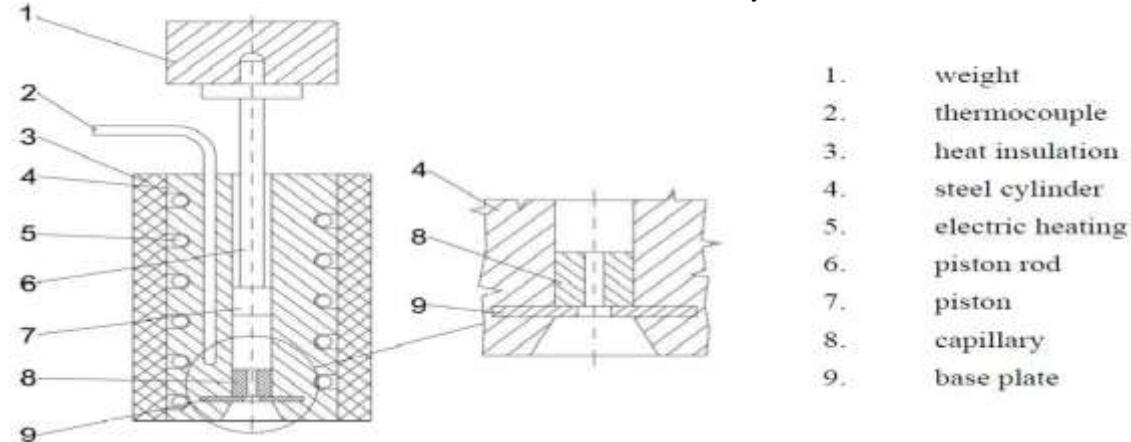


Figure .1 Typical apparatus for determining melt flow rate (showing one of the possible methods of retaining the die and one type of piston) (2).

Vol. 9 Issue 9 September - 2025, Pages: 1-12

Z. Testing Procedure:

A small amount of the polymer sample around 4g for (LDPE) and 6 grams for (PP) is taken in the specially designed MFI apparatus. The apparatus consists of a small die inserted into the apparatus, with the outside diameter is 9.475mm, inner diameter is 2.095 mm and the length of die is 8.000mm.

The material is packed properly inside the barrel to avoid formation of air pockets. A piston is introduced which acts as the medium that causes extrusion of the molten polymer. The length of piston bar is 210mm; piston diameter is 9.475mm.

The sample is preheated for a specified amount of time: 5 min at 190°C for polyethylene and 6 min at 230°C for polypropylene. After the preheating a specified weight is introduced into the piston. Examples of standard weights are 2.16 kg to 5 kg. The weight exerts a force on the molten polymer and it immediately starts flowing through the die. A sample of the melt is taken after desired period of time and is weighed accurately.MFI is expressed as grams of polymer/10 minutes of total time of the test. {Synonyms of Melt Flow Index are Melt Flow Rate and Melt Index. More commonly used are their abbreviations: MFI, MFR and {MI}. Confusingly, MFR may also indicate "melt flow ratio", the ratio between two melt flow rates at different gravimetric weights. More accurately, this should be reported as FRR (flow rate ratio), or simply flow ratio. FRR is commonly used as an indication of the way in which rheological behavior is influenced by the molecular mass distribution of the material. MFI is often used to determine how a polymer will process. However MFI takes no account of the shear, shear rate or shear history and as such is not a good measure of the processing window of a polymer. The MFI device is not an extruder in the conventional polymer processing sense in that there is no screw to compress heat and shear the polymer. MFI additionally does not take account of long chain branching nor the differences between shear and elongation rheology. Therefore two polymers with the same MFI will not behave the same under any given processing conditions.

3-1-Techniques used to calculate mass flow \dot{V} , volume flow \dot{V} , viscosity η , maximum shear stress τ_f and maximum shear rate $\dot{\gamma}_f$:

Most processing technologies of thermoplastic polymers have a phase when the material is in a fluidic state before formation. This makes possible the completion of formation with relatively small force and pressure. The knowledge of behavior and characteristics of melts and the basics of melt rheology are essential for plastic processing and manufacturing of polymer products 3.2. Basics, viscosity law of Newton (3):

What is the difference between solids and fluids? To the right a fluid layer can be seen placed between two similar plates. The cross section of the solid body and fluid parallel with the plates is marked with A $[m^2]$. The lower plate is immobile while the upper one can be moved in parallel. If an F [N] force is applied on the upper plate, a τ =F/A [Pa] shear stress is developed and deformation occurs in the solid body. The γ angle featuring the deformation is directly proportional with the τ [Pa] shear stress to a certain limit (Hooke law, Chapter one section {1-2-1} Figure 1-3A.). Thus the deformation is proportional with the shear stress developing in the solid body and the proportionality coefficient is the G shear elasticity modulus

$$G = \frac{\tau}{\nu}.$$
 (1)

If there is fluid between the plates, the upper plate moves with a u velocity induced by the F force, the fluid is under a continuous deformation. Thus in case of fluids shear rate (dy/dt) is examined instead of γ deformation. The basics of fluid mechanics according to Newton model is introduced below. The Newton model used for describing the behavior of real fluids is the basic model of melt rheology. In case of Newtonian fluids the velocity distribution is linear between the two plates. The velocity of fluid particles near to the stationary plate is vx = 0, while near to the upper plate the flow velocity is equal with the u velocity of the plate. Let's determine the dy rotatation of the M line during a dt time period! The upper end of the line is moving with a velocity of vx + t(dvx/dy)dy, while the lower end is moving with a velocity of vx. We can get the rotation (dy) belonging to dt duration by dividing the difference of length of path with dy. The time specific angular rotation, i.e. the shear rate is given by dividing with dt: $\dot{\gamma} = \frac{d\gamma}{dt} = \frac{dv_x}{dy} \qquad (2)$

$$\dot{\gamma} = \frac{d\gamma}{dt} = \frac{dv_x}{dv} \tag{2}$$

We can determine the linear relationship between shear rate and shear stress, the Newton equation, where $\eta [Pa \cdot s]$ is a factor depending on fluid properties called dynamic viscosity: $\tau = \eta \dot{\gamma} = \eta \frac{d\gamma}{dt} = \eta \frac{dv_x}{dy} \ \eqno(3)$

$$\tau = \eta \dot{\gamma} = \eta \frac{d\gamma}{dt} = \eta \frac{dv_x}{dv} \qquad (3)$$

The value of η depends on the shear stress required for maintaining a certain shear rate in case of a given fluid. It should be noted that if $\dot{\gamma}$ & shear rate converges to zero, shear stress also converges to zero. This means that the static friction of fluids – in spite of solid materials – is zero. Another difference is that fluids can be deformed endlessly without the alteration of their structure.

The flow velocity of fluids near to a wall is equal with the velocity of the wall. This phenomenon is called the law of adherence.

3.3. Flow in capillary (3):

The following chapter is dealing with flow of Newtonian fluids in a small diameter tube, i.e. capillary, because in the viscometer the tested material must pass through a capillary. Figure 3-4 shows the schema of capillary.

Equation (3) and the fact that $\dot{\gamma}$ shear rate can be expressed with the derivative function of flow velocity:

$$\tau = \, \eta \dot{\gamma} = \, \eta \, \frac{\mathrm{d} v(r)}{\mathrm{d} r} \quad \tag{4}$$

Where v(r) [m/s] is the flow velocity of the melt in the function of radial location r [m] is the radial coordinate of capillary, $(0 \le 1)^n$ $r \leq R$).

From equation (3.4):

In order to continue the development we have to determine the distribution of
$$\tau$$
 shear stress along the cross section of the capillary.

The following equation describes the force equilibrium of a fluid element in the function of r radius of the capillary:

$$2\pi r l \tau = r^2 \pi \Delta p \qquad (6)$$

Where Δp [Pa] is the pressure difference between the inlet (A_{in}) and outlet (A_{out}) cross section of the capillary, l(m) is the length of the capillary. The force developing on the surface of r radius cylindrical shell is in equilibrium with the pressure on the r radius base circle of the cylinder $(0 \le r \le R)$.

Furthermore we assume that the pressure decrease along the capillary axis (Figure 3-4) is linear, thus τ , ν and $\dot{\gamma}$ & are functions of the radius but they do not change along the capillary axis. From equation (3.6) we get the function describing the distribution of τ in the cross section, which is independent on the material and depends only on the loading and the dimensions of the capillary:

$$\tau = \frac{\Delta p}{2l} r \dots (7)$$

 $\tau = \frac{\Delta p}{2l} r \qquad (7)$ The distribution has a conical shape; it is stress-free in the axis and reaches its maximum value at r = R. The τ shear stress is directly proportional with the radius, thus it reaches its maximum value at the wall of the capillary, at r = R (Figure 3-5).

proportional with the radius, thus it reaches its maximum value at the war of the capitally,
$$\tau = \tau_{r=R} = \tau_f = \frac{\Delta p}{2l} R(8)$$
By substituting equation (3.7) into (3.5) we get the following differential equation:
$$\frac{dv}{dr} = \frac{\Delta p}{2l\eta} r(9)$$

$$\frac{\mathrm{d}\mathbf{v}}{\mathrm{d}\mathbf{r}} = \frac{\Delta \mathbf{p}}{2l\mathbf{n}} \mathbf{r} \tag{9}$$

From differential equation (3.9):

$$d\mathbf{v} = \frac{\Delta \mathbf{p}}{2 \ln r} \mathbf{r} \, \mathbf{d}_{\mathbf{r}} \, \dots \tag{10}$$

From (3.10) by integration

$$v = \frac{\Delta p}{2l\eta} \frac{r^2}{2} + c$$
 (11)

In order to determine constant c we shall use the following boundary condition:

At
$$r = R$$
: $v = 0$ (12)

By substituting the above equation into (3.11):

$$0 = \frac{\Delta p}{2 l \eta} \frac{R^2}{2} + c$$
 (13)

From equation (3.13) we get the value of c:
$$c = -\frac{\Delta pR^2}{4 l \eta} . \tag{14}$$
By substituting the value of constant c into equation (3.11) we get the function describing the distribution

By substituting the value of constant c into equation (3.11) we get the function describing the distribution of flow velocity in the cross section (Figure 3-5):

$$v = \frac{\Delta p}{4 l \eta} (r^2 - R^2) \le 0 \qquad (15)$$

This is a paraboloid velocity distribution. The negative sign originates from the fact that the flow direction and the direction of pressure growth are opposite. In practice the velocity distribution is calculated from the following equation: $v = \frac{\Delta p}{4 l \eta} (R^2 - r^2) \dots (16)$

$$v = \frac{\Delta p}{4 \ln n} (R^2 - r^2)$$
 (16)

3.4 Evaluation of standard test (2)

The instrument is able to determine Melt Flow Index (MFI) by measuring the mass of melt which can be calculated by the following equation:

 $T \ [^{\circ}C]$; Test temperature,

F [*N*]; Weight force,

s [-]; Factor of standard time (10 minutes = 600 s), s = 600

t [s]; Time needed for V amount of material to flow through the capillary,

m[g]; Amount of material flowing through the capillary under t time.

To determine MVR (Melt Volume Rate) volume rate, this can be calculated by the following equation:

$$MVR_{(T,F)} = \frac{v.s}{t}$$
 (18)

Where: $MVR [cm^3/10 min]$; volume rate,

 $T \ [^{\circ}C]$; Test temperature,

F[N]; Weight force,

S [-]; factor of standard time (10 minutes = 600 s), s = 600

t [s]; Time needed for V amount of material to flow through the capillary,

 $V[cm^3]$; Amount of material flowing through the capillary under t time.

3.4.1Evaluation of MFI test (4):

In case of MFI tests, we apply a simplification, namely we neglect the pseudoplastic behavior of the polymer melt and we treat it as a Newtonian fluid. The data required for drawing the viscosity curve can be calculated the following way:

 \dot{V} & $[m^3/s]$ volume flow can be calculated from the MVR by the following equation:

$$\dot{\mathbf{V}} = \frac{\mathsf{MVR}}{\mathsf{S}_10^6} \tag{19}$$

Where:

 \dot{V} [m^3/s]; volume flow,

MVR [$cm^3/10$ min]; volume flow measured by instrument,

s [-]; factor of standard time (10 minutes = 600 s), s = 600

Division with 10^6 is needed to convert $[cm^3]$ to $[m^3]$.

MFI can be calculated by equation (3.17).

 \dot{G} [kg/s] mass flow can be calculated from the MFI by the following equation:

$$\dot{G} = \frac{MFI}{S \cdot 10^3} \tag{20}$$

Where:

 \dot{G} [kg/s]; mass flow,

MFI [g/10 min]; melt flow index,

s [-]; factor of standard time (10 minutes = 600 s), s = 600 s

Division with 10^3 is needed to convert [g] to [kg].

 ρ [kg/m3] density of the melt flow rate can be calculated from $\dot{V}\&\dot{G}$ volume flow and mass flow:

$$\rho = \frac{m}{0.711 L} = \frac{\dot{G}}{\dot{V}}....(21)$$

Where:

L [cm]: piston moved distance or average distance of the measurement,

m [g]: the sample quality of extrusion when the piston moved L [cm].

Pressure at inlet cross section of the capillary can be approximated with the pressure Calculated from D diameter of piston and F force of weight:

$$\Delta p = \frac{4}{\pi D^2} F \tag{22}$$

Furthermore we assume that according to Figure 3-4 Pressure decreasing is linear along the capillary axis, thus τ and $\dot{\gamma}$ depends on radius but is constant along the capillary axis.

$$\tau_{\text{max}} = \tau_{\text{r=R}} = \tau_{\text{f}} = \frac{\Delta p}{2l} R \dots (23)$$

Dynamic viscosity (η) can be calculated by:

$$\mu = \frac{\pi \Delta p.R^4}{8l\dot{V}} \qquad (24)$$
 The distribution of $\dot{\gamma}$ shear rate in the cross section:

$$\dot{\gamma} = \frac{\tau}{\mu} = \frac{\Delta p}{2\mu l} r \dots (25)$$

The distribution of $\dot{\gamma}$ has a shape similar to the τ , because they differ only in a constant factor. $\dot{\gamma}$ Reaches its maximum value at the capillary wall.

$$\dot{\gamma}_{\text{max}} = \dot{\gamma}_{r=R} = \frac{\Delta p}{2\mu l} R = \frac{\tau_f}{\mu} = \dot{\gamma}_f \dots (26)$$

4. RESULT AND DISSCUSION

1. Melt Flow Index (MFI) and Melt Volume Rate (MVR)

The measured values of MFI and MVR for LDPE and PP under different test conditions are summarized in Table 1. As expected, both polymers exhibited higher MFI and MVR with increasing temperature and applied load. This behavior reflects the reduction in melt viscosity due to thermal softening and enhanced chain mobility.

Table 1. MFI and MVR values of LDPE and PP under different test conditions

Polymer	Temp (°C)	Load (kg)	MFI (g/10 min)	MVR (cm ³ /10 min)
LDPE	170	2.16	0.74	0.80
LDPE	190	2.16	1.85	2.00
LDPE	210	2.16	3.61	3.91
PP	190	2.16	1.23	1.53
PP	210	2.16	2.72	3.39
PP	230	2.16	5.80	7.23

2. Shear Stress and Shear Rate

Using the MFI data, the apparent shear stress (τ) and shear rate (γ) were calculated and are presented in **Table 2**. Both LDPE and PP showed shear-thinning characteristics, where viscosity decreased as shear rate increased. LDPE generally exhibited lower shear stress values compared to PP under the same conditions.

Table 2. Shear stress and shear rate values calculated from MFI

Polymer	Temp (°C)	Load (kg)	τ (Pa)	$\dot{\gamma}$ (s ⁻¹)
LDPE	170	2.16	489.0	37.72
LDPE	190	2.16	489.0	94.32
LDPE	210	2.16	489.0	184.02
PP	190	2.16	489.0	62.56
PP	210	2.16	489.0	138.23
PP	230	2.16	489.0	294.88

3. Apparent Viscosity

The apparent viscosity (η) values derived from MFI are shown in **Table 3**. Both polymers displayed significant viscosity reduction with increasing temperature, confirming the strong thermal sensitivity of polyolefin melts.

Table 3. Apparent viscosity values of LDPE and PP

Polymer	Temp (°C)	Load (kg)	η (Pa·s)
LDPE	170	2.16	12.97
LDPE	190	2.16	5.19
LDPE	210	2.16	2.66
PP	190	2.16	7.82
PP	210	2.16	3.54
PP	230	2.16	1.66

4. Rheological Modeling

The experimental data were fitted with the Power Law and Carreau models. The flow behavior index (n) for LDPE ranged from 0.58-0.61, while for PP it ranged from 0.60-0.66. These values confirm pseudoplastic non-Newtonian behavior (n < 1). The Carreau model provided a better fit across a wider shear rate range.

5. Activation Energy of Flow

Arrhenius-type analysis of viscosity as a function of reciprocal temperature showed that PP has a higher activation energy for viscous flow compared to LDPE. This indicates that PP viscosity is more sensitive to thermal changes, requiring tighter temperature control during processing.

5. Discussion

The findings confirm that MFI can serve as an effective empirical tool to capture key rheological trends, such as shear-thinning, temperature sensitivity, and processing stability. Although MFI is not a fundamental property, its strong correlation with viscosity and flow behavior justifies its application in quality control and process optimization for thermoplastic polymers.[12].

6. Conclusion

This study investigated the rheological behavior of low-density polyethylene (LDPE) and polypropylene (PP) using melt flow index (MFI) measurements under various temperatures and applied loads[10]. The results demonstrated a clear decrease in apparent viscosity with increasing temperature and load, confirming the pseudoplastic non-Newtonian behavior of both polymers. LDPE exhibited lower shear stress and viscosity compared to PP, indicating its higher processability at comparable conditions. Rheological

International Journal of Academic Engineering Research (IJAER)

ISSN: 2643-9085

Vol. 9 Issue 9 September - 2025, Pages: 1-12

modeling using Power Law and Carreau equations provided accurate fits for experimental data, while activation energy analysis revealed that PP is more sensitive to temperature changes than LDPE. Overall, the findings highlight the effectiveness of MFI as a practical, rapid tool for evaluating polymer processability and predicting rheological behavior in industrial applications.

References

- [1] Mertz R, Müller M, Reiter G. Melt flow index and its correlation with polymer rheology and molecular weight distribution. Polymer Testing. 2013;32(8):1584–1592.
- [2] Traxler A, Klein R, Hoffmann T. Predictive models for MFR and shear viscosity of polypropylene blends using Arrhenius and Cragoe equations. J Appl Polymer Sci. 2024;141(12):e52678.
- [3] Polymer Lifecycle. Operational parameters influencing MFI and viscosity in recycled polypropylene. Polymer Lifecycle. 2025;4(1):55–72.
- [4] Kumar A, Rao P. Correlation between MFI and rheological properties of recycled polyethylene films. Appl Rheol. 2024;34(2):215–227.
- [5] García M, Torres A, Martínez J. Non-Newtonian behavior of HDPE and PP: Power law modeling in extrusion. Manuf Technol. 2023;23(4):415–424.
- [6] Fang X, Huang L. Shear and elongational rheology of recycled polyethylene: A comparison with MFI trends. J Rheol. 2024;68(1):55–68.
- [7] Zhiltsova O, Oliveira M. Recycled PP blends: Processing performance and MFI predictability. Polymers. 2025;17(4):765–776.
- [8] Chen Y, Wang J, Liu H. Thermomechanical degradation of LDPE and PP during multiple extrusion cycles: Impact on MFI and viscosity. Polym Degrad Stab. 2024;210:110332.
- [9] Patel D, Sharma V, Singh R. Effect of glass fiber reinforcement on MFI and viscosity of recycled polypropylene composites. Compos Interfaces. 2024;31(6):545–558.
- [10] Zhang Q, Xu Z, Li Y. Kinetic modeling of polypropylene degradation: Linking molecular weight changes to MFI. Macromol React Eng. 2025;19(3):e2300021.
- [11] Park J, Lee K, Cho H. Temperature sensitivity of polypropylene melt viscosity: An Arrhenius-type analysis. J Therm Anal Calorim. 2023;147(7):4931–4942.
- [12] Santos A, Mendes J. Molecular weight distribution and its impact on MFI of polypropylene. Polym Eng Sci.

APPENDICES(A)

(Low density polyethylene)

Table (1)Measured melt flow index for LDPE at 170 °C

	Measured Results							
Sample	Load (Kg)	Force (N)	Length (mm)	Time (Sec)	Mass average (g)	$MFI \ (g/10min)$	Density (Kg/m^3)	MVR (cm ³ /10min)
1	2.16	21.19	5.14	60	0.097	0.97	798	1.22
2	2.40	23.54	6.40	60	.0.12	1.20	791	1.52
3	2.84	27.86	7.33	60	0.153	1.53	885	1.73
4	3.36	32.96	10.94	60	0.20	2.00	771	2.59
5	3.80	37.28	12.57	60	0.25	2.50	839	2.98
6	5.00	49.05	20.57	60	0.40	4.00	821	4.87

Table(.2)Measured melt flow index for LDPE at 190 °C

	Measured Results							
Sample	Load (Kg)	Force (N)	Length (mm)	Time (Sec)	Mass average (g)	$MFI \\ (g/10min)$	Density (Kg/m^3)	MVR (cm ³ /10min)
1	2.16	21.19	9.74	60	0.18	1.8	779	2.31
2	2.40	23.54	12.75	60	0.22	2.2	730	3.02
3	2.84	27.86	16.66	60	0.28	2.8	710	3.95
4	3.36	32.96	21.57	60	0.37	3.7	724	5.11
5	3.80	37.28	26.55	60	0.45	4.5	714	6.29
6	5.00	49.05	40.57	60	0.73	7.3	761	9.62

Table (3)Measured melt flow index for LDPE at 210 °C

	Measured Results							
Sample	Load (Kg)	Force (N)	Length (mm)	Time (Sec)	Mass average (g)	$rac{ ext{MFI}}{(g/10min)}$	Density (Kg/m^3)	MVR (cm ³ /10min)
1	2.16	21.19	17.08	60	0.32	3.2	780	4.10
2	2.40	23.54	25.37	60	0.39	3.9	639	6.10
3	2.84	27.86	30.00	60	0.53	5.3	746	7.10
4	3.36	32.96	41.46	60	0.65	6.5	665	9.76
5	3.80	37.28	52.97	60	0.95	9.5	759	12.50
6	5.00	49.05	51.81	60	1.35	13.5	732	18.44

Table (4)) Calculated	Results	of LDPE a	it 170 °C

	Table (4) Calculated Results of EDI E at 170 C							
	Calculated Results							
C 1	T -	1 77	÷			ı		
Sample	Force	V	G	Δp	$ au_{ m f}$	η	γ	
	(N)	$10^{-9}(\frac{\text{m}^3}{\text{s}})$	$10^{-6}(\frac{\text{kg}}{\text{s}})$	(Mp _a)	(Mp _a)	(Mp _a)	(S^{-1})	
1	21.19	2.03	1.62	0.300	0.01965	0.00873	2.251	
2	23.54	2.53	2.00	0.333	0.02181	0.00777	2.807	
3	27.86	2.88	2.55	0.395	0.02587	0.00810	3.194	
4	32.96	4.32	3.33	0.467	0.03059	0.00639	4.787	
5	37.28	4.97	4.17	0.529	0.03465	0.00629	5.509	
6	49.05	8.12	6.67	0.696	0.04559	0.00506	9.009	

Table (5) Calculated Results of LDPE at 190 °C

	Calculated Results						
Sample	Force (N)	$\frac{\dot{V}}{10^{-9}(\frac{m^3}{s})}$	$\frac{\dot{G}}{10^{-6}(\frac{kg}{s})}$	Δp (Mp _a)	$ au_{\mathrm{f}} ag{Mp_{\mathrm{a}}}$	η (Mp _a)	ý (S ⁻¹)
1	21.19	3.85	3.00	0.300	0.01965	0.00460	4.27
2	23.54	5.03	3.67	0.333	0.02181	0.00391	5.58
3	27.86	6.58	4.67	0.395	0.02587	0.00354	7.25
4	32.96	8.52	6.17	0.467	0.03059	0.00323	9.47
5	37.28	10.50	7.50	0.529	0.03465	0.00292	11.67
6	49.05	16.00	12.17	0.696	0.04559	0.00256	17.81

Table (6) Calculated Results of LDPE at 210 °C

		14010 (0	Calculated Res		210		
Sample	Force	Ż	Ġ	Δр	$ au_{ m f}$	η	Ϋ́
	(N)	m^{3}	$10^{-6} \left(\frac{\text{kg}}{-} \right)$	(Mp_a)	(Mp_a)	(Mp_a)	(S^{-1})
		$10^{-9}(\frac{m}{s})$	10 °(<u>—</u>)				
1	21.19	6.83	5.33	0.300	0.01965	0.00259	7.59
2	23.54	10.17	6.50	0.333	0.02181	0.00193	11.30
3	27.86	11.83	8.83	0.395	0.02587	0.00197	13.13
4	32.96	16.27	10.83	0.467	0.03059	0.00169	18.10
5	37.28	20.83	15.83	0.529	0.03465	0.00149	23.26
6	49.05	30.73	22.50	0.696	0.04559	0.00133	43.28

Table (7) to calculate the activation energy of LDPE at different temperature

	A	η_0 Pa.S	K^{-1}	R^2
LDPE at 1700C $\eta_0 = 9986 e^{-0.07\dot{\gamma}}$	9986	7328.17	2.257	0.946
LDPE at 190° C $\eta_0 = 4954 e^{-0.04\dot{\gamma}}$	4954	3462.17	2.160	0.912
LDPE at 210^{0} C $\eta_{0} = 2687 e^{-0.02\dot{\gamma}}$	2687	1905.33	2.070	0.868

Table (8) to calculate the viscosity of LDPE by using power law at different temperature. Power Law : $\eta = \bar{K}\dot{\gamma}^{n-1}$

Material	η	\overline{K}	n
LDPE at 170°C	12092γ˙ ^{-0.39}	12092	0.61
LDPE at 190°C	7937γ̇ ^{-0.39}	7937	0.61
LDPE at 210°C	$5868\dot{\gamma}^{-0.42}$	5868	0.58

Table (9) to calculate the viscosity of LDPE by using carreau model at different temperature.

Carreau model:
$$\eta_a = \eta_0 * a_T \left[1 + a_T (A_t * \dot{\gamma}_a)^2 \right]^{\frac{n-1}{n}}$$

$$\log aT = \frac{C_1 (T_1 - T_0)}{C_2 + (T_1 - T_0)} - \frac{C_1 (T_2 - T_0)}{C_2 + (T_2 - T_0)}$$

Material	η_0 Pa.S	a_T	A_t	n
LDPE at 170°C	5060	0.716	0.111	0.61
LDPE at 190°C	2560	0.741	0.056	0.61
LDPE at 210°C	1330	0.764	0.029	0.58

APPENDICES(B) (Polypropylene)

Table (10)Measured melt flow index for PP at 190 °C

	Measured Results								
Sample	Load (Kg)	Force (N)	Length (mm)	Time (Sec)	Mass average (g)	MFI $(g/10min)$	Density (Kg/m^3)	MVR (cm ³ /10min)	
1	1.2	11.77	3.72	10	0.063	3.80	722	5.26	
2	1.285	12.60	4.20	10	0.073	4.38	739	5.93	
3	1.525	14.96	5.65	10	0.090	5.40	673	8.02	
4	1.965	19.27	7.98	10	0.133	7.98	706	11.30	
5	2.16	21.19	9.53	10	0.153	9.18	680	13.50	
6	2.40	23.54	10.77	10	0.180	10.80	697	15.30	
7	2.84	27.86	13.10	10	0.230	13.80	753	18.33	
8	3.36	32.96	18.80	10	0.317	19.02	712	26.71	

Table (11)Measured melt flow index for PP at 210 °C

	Measured Results								
Sample	Load (Kg)	Force (N)	Length (mm)	Time (Sec)	Mass average (g)	MFI $(g/10min)$	Density (Kg/m^3)	MVR (cm ³ /10min)	
1	1.2	11.77	2.88	5	0.053	6.36	781	8.10	
2	1.285	12.60	3.70	5	0.060	7.20	684	10.50	
3	1.525	14.96	4.60	5	0.083	9.96	764	13.09	
4	1.965	19.27	7.28	5	0.107	12.84	718	20.70	
5	2.16	21.19	8.23	5	0.120	14.40	615	23.40	
6	2.40	23.54	10.16	5	0.147	17.64	609	28.90	
7	2.84	27.86	11.80	5	0.197	23.64	703	33.59	
8	3.36	32.96	15.22	5	0.250	30.00	693	43.30	

Table (12)Measured melt flow index for PP at 230 0 C

	Measured Results								
Sample	Load (Kg)	Force (N)	Length (mm)	Time (Sec)	Mass average (g)	MFI $(g/10min)$	Density (Kg/m^3)	MVR (cm ³ /10min)	
1	1.2	11.77	4.75	5	0.077	9.20	680	13.52	
2	1.285	12.60	4.83	5	0.080	9.60	698	13.75	
3	1.525	14.96	5.73	5	0.100	12.00	735	16.31	
4	1.965	19.27	10.11	5	0.177	21.20	738	28.78	
5	2.16	21.19	12.14	5	0.200	24.00	695	34.55	
6	2.40	23.54	13.70	5	0.220	26.40	676	38.99	

Table (13) Calculated Results of PP at 190 °C

	Calculated Results								
Sample	Force	Ż	Ġ	Δр	$ au_{ m f}$	η	Ϋ́		
	(N)	m^3	$10^{-6} (\frac{\text{kg}}{-})$	(Mp_a)	(Mp_a)	(Mp_a)	(S^{-1})		
		$10^{-9}(\frac{m}{s})$	10 °()						
1	11.77	8.77	6.33	0.167	0.0109	0.001125	9.69		
2	12.60	9.88	7.30	0.178	0.0117	0.001065	10.99		
3	14.96	13.37	9.00	0.212	0.0139	0.000937	14.83		
4	19.27	18.83	13.30	0.273	0.0179	0.000857	20.89		
5	21.19	22.50	15.30	0.300	0.0196	0.000788	24.87		
6	23.54	25.83	18.00	0.334	0.0219	0.000774	28.29		
7	27.86	30.55	23.00	0.395	0.0259	0.000764	33.90		
8	32.96	44.52	31.70	0.467	0.0306	0.000619	49.43		

Table (14)Calculated Results of PP at 210 °C

	Table (14) Calculated Results of 11 at 210 C								
	Calculated Results								
Sample	Force	Ÿ	Ġ	Δр	$ au_{ m f}$	η	Ϋ́		
	(N)	$_{\circ}$ m^{3}	$10^{-6} (\frac{\text{kg}}{-})$	(Mp_a)	(Mp_a)	(Mp_a)	(S^{-1})		
		$10^{-9}(\frac{\text{m}^3}{\text{s}})$	$10^{-6}(\frac{-1}{s})$						
1	11.77	13.50	10.6	0.167	0.0109	0.000731	14.9		
2	12.60	17.50	12.0	0.178	0.0117	0.000601	19.5		
3	14.96	21.68	16.6	0.212	0.0139	0.000578	24.0		
4	19.27	34.57	21.4	0.273	0.0179	0.000467	38.3		
5	21.19	38.97	24.0	0.300	0.0196	0.000455	43.1		
6	23.54	48.28	29.4	0.334	0.0219	0.000409	53.5		
7	27.86	55.97	39.4	0.395	0.0259	0.000417	62.1		
8	32.96	72.05	50.0	0.467	0.0306	0.000383	79.9		

	Table (13) Calculated Results of 11 at 250 C									
	Calculated Results									
Sample	Force	Ÿ	Ġ	Δр	$ au_{ m f}$	η	Ϋ́			
	(N)	m^3	kg	(Mp_a)	(Mp_a)	(Mp_a)	(S^{-1})			
	` /	$10^{-9}(\frac{m^3}{s})$	$10^{-6} \left(\frac{\text{kg}}{\text{c}} \right)$	\ ray	(Fa)	\ Fa7	(-)			
		S	S							
1	21.19	22.62	15.4	0.300	0.01965	0.000436	25.00			
	22.54	22.00	160	0.222	0.00101	0.000450	25.40			
2	23.54	22.88	16.0	0.333	0.02181	0.000459	25.49			
3	27.86	27.17	20.0	0.395	0.02587	0.000461	30.15			
4	32.96	48.03	35.4	0.467	0.03059	0.000336	53.27			
5	37.28	57.47	40.0	0.529	0.03465	0.000309	63.43			
6	49.05	64.98	44.0	0.696	0.04559	0.000304	72.04			

Table (16) to calculate the viscosity of PP by using power law at different temperature Power Law: $\eta = \overline{K}\dot{\gamma}^{n-1}$

Material	η	\overline{K}	n
PP at 190°C	$2421\dot{\gamma}^{-0.34}$	2421	0.66
PP at 210°C	$1903\dot{\gamma}^{-0.37}$	1903	0.63
PP at 230°C	PP at 230 ⁰ C 1715γ˙ ^{-0.42}		0.60

Table (17) to calculate the viscosity of PP by using carreau model at different temperature

Carreau model:
$$\eta_a = \eta_0 * a_T [1 + a_T (A_t * \dot{\gamma}_a)^2]^{\frac{n-1}{n}}$$

$$\log aT = \frac{C_1 (T_1 - T_0)}{C_2 + (T_1 - T_0)} - \frac{C_1 (T_2 - T_0)}{C_2 + (T_2 - T_0)}$$

Material	η_0 Pa.S	a_T	A_t	n
PP at 190°C	619	0.546	0.020	0.66
PP at 210°C	383	0.593	0.0125	0.63
PP at 230°C	304	0.634	0.0139	0.60